Frontiers in Bioscience Landmark

Front. Biosci. (Landmark Ed) **2022**; 27(7): 216
https://doi.org/10.31083/j.fbl2707216

Original Research

Anoctamin 1 Inhibition Suppresses Cystogenesis by Enhancing Ciliogenesis and the Ciliary Dosage of Polycystins

Tao Xu[1,2], Meihan Chen[2,3], Qingwen Xu[4], Cheng Xue[2], Lili Fu[2], Kun Ling[4], Jinghua Hu[4], Changlin Mei[2,*]

[1]Department of Nephrology, Shanghai Jiaotong University Medical School affiliated Shanghai Sixth People's Hospital, 200233 Shanghai, China
[2]Division of Nephrology, Kidney Institution of Chinese People's Liberation Army, Changzheng Hospital, 200003 Shanghai, China
[3]Department of Nephrology and Rheumatology, Shanghai Tenth People's Hospital, Tongji University School of Medicine, 200003 Shanghai, China
[4]Department of Biochemistry and Molecular Biology, Mayo Clinic, Rochester, MN 55902, USA
*Correspondence: changlinmei@smmu.edu.cn (Changlin Mei)
Academic Editor: Josef Jampílek
Submitted: 21 April 2022 Revised: 31 May 2022 Accepted: 27 June 2022 Published: 8 July 2022

Abstract

Background: Autosomal dominant polycystic kidney disease (ADPKD) is a ciliopathy characterized by abnormal tubular epithelial proliferation and fluid secretion. Anoctamin 1 (ANO1) is a calcium-dependent chloride channel. However, how ANO1 contributes to ADPKD is largely unexplored. **Methods**: Kidney tissues from ADPKD patients, *Pkd1*$^{RC/RC}$ mice model, WT9-7 human *PKD1*$^{+/-}$ cells, and 3D culture models *in vitro* were used. Localization of ANO1 and cilium length were investigated by confocal immunofluorescence. **Results**: We found that ANO1 was consistently upregulated in human and mouse PKD kidneys. Intriguingly, ANO1 located in a vesicle-like pattern at the ciliary base but not on the ciliary surface. ANO1 deficiency enhanced ciliogenesis and the ciliary dosage of polycystin-2 in human PKD cells, and reduced cyst formation in 3D culture models. Moreover, inhibition of ANO1 abolished the activation of STAT3 and ERK pathways in PKD cells. **Conclusions**: Our data indicate ANO1 is a negative regulator for both cilia length and cilia trafficking of polycystin-2 and provide mechanistic insights regarding the therapeutic potential of ANO1 pathway in ADPKD treatment.

Keywords: autosomal dominant polycystic kidney disease; anoctamin 1; primary cilium; polycystin

1. Introduction

Autosomal dominant polycystic kidney disease (ADPKD) is the most common hereditary kidney disease and is a leading cause of end-stage kidney disease with an incidence of 1 in 1000 individuals [1]. ADPKD is mainly caused by mutations in *PKD1* (encoding polycystin 1, PC1) or *PKD2* (encoding polycystin 2, PC2) gene, and in GANAB (glucosidase ii alpha subunit), DNAJB11, ALG9, or IFT140 for the rest 10% [2]. PC1 and PC2 are located in the primary cilium. Proper targeting of polycystins to the ciliary surface is critical for polycystin function [3,4]. ADPKD is considered a cilia-related disease [5]. According to one of the theories in ADPKD, the complex of PC1/PC2 acts as a mechanical sensor on the ciliary surface of epithelial cells lining renal tubules to regulate the proper response to intra-tubular liquid flow through triggering a Ca^{2+} influx [6,7].

Renal cysts form when the level of functional PC1 or PC2 drops below a critical threshold, with the primary cilium of renal epithelial cells as a major functional site [8]. Accumulating evidence in human genetics and hypomorphic rodent models also showed that the severity of ADPKD is negatively correlated with the dosage of functional polycystins [9–12]. Besides, ADPKD is characterized by aberrant proliferation of tubular epithelial cells, which is accompanied by activation of multiple cell proliferation signaling pathways such as STAT3 and ERK pathways [11,12].

Anoctamin 1 (ANO1) is a newly identified calcium-dependent chloride channel, which has recently been shown to be implicated in cystic fluid secretion *in vitro* [13–15]. Inhibition of ANO1, either pharmacological or genetical, effectively suppressed cystogenesis in *Pkd1*$^{-/-}$ conditional knockout mice [16]. It has been reported that ANO1 is required for ciliogenesis or maintenance of primary cilia [17,18]. The correlation between ANO1 and human PKD, as well as the molecular mechanism underlying pro-cystic action of ANO1, is poorly understood. Here, we discovered that ANO1 is abnormally upregulated in cystic lining cells in human and mouse PKD kidneys, and also in mouse PKD models. We further revealed the subcellular localization of ANO1 in the context of cilia and its important role in regulating ciliogenesis and polycystin trafficking. ANO1 inhibition effectively suppressed both cystogenesis *in vitro* cystogenesis model and dysregulated proliferative pathways in human PKD cells.

2. Materials and Methods

2.1 Human Samples

Kidney specimens of seven patients (four males, three females; 57.7 ± 9.1 years of age (mean ± s.d.); four ADPKD patients and three renal cell carcinoma patients with relatively normal renal tissue) were obtained from

Changzheng Hospital, Shanghai, China. Three patients were receiving hemodialysis at the time of nephrectomy, thus representing rather late stages of ADPKD. Collection and analysis of tissue samples were approved by the local ethics committee. This study was conducted in accordance with the Declaration of Helsinki.

2.2 Animals

Animal experiments were approved by the local institutional review board for the care of animals and were performed in accordance with National Institutes of Health guidelines. *PKD1*$^{RC/RC}$ mice (provided by Dr. Peter Harris) were housed on a 12:12-h light–dark cycle under constant temperature (24 $\pm$ 1.1 °C) in standard cages, fed with a standard diet, and had free access to tap water in Mayo Clinic experimental animal center.

2.3 Cell Culture

Madin-Darby canine kidney (MDCK) cells, inner-medullary collecting duct (IMCD3) cells, *PKD1*$^{+/-}$cells and *GANAB* cells (from the lab of Dr. Peter Harris) were grown on glass coverslips in DMEM (Dulbecco's Modified Eagle Medium) supplemented with 10% fetal bovine serum at 37 °C in a humidified incubator containing 5% CO_2 until full confluence. Cells were subjected to serum starvation to induce cilia growth. The medium was supplemented with forskolin and either Tinh16-A01 (5 μM) or Tannic acid (5 μM) as ANO1 inhibitors. The medium was changed every 24–48 h.

To knock down ANO1, RCTE or *GANAB* cells were transfected with 50 nM siRNA using Lipofectamine RNAiMAX (No. 13778075, Invitrogen, Carlsbad, USA) following the manufacturer's instructions. siRNA sequences targeting human ANO1 are as follows: siRNA1,5′-GAAGCAACACCTATTCGACCTG -3′; and siRNA2:5′-TCCGTAACTTGCCCATTCCTC -3′.

Lentivirus system was used to construct stabilized Ano1 knock-down MDCK cell lines. Short hairpin RNA (shRNA)-expressing lentivirus constructs were generated using pLV-RNAi vector (Biosettia, San Diego, CA, USA. The following shRNA sequence was used to target Canis lupus ANO1: 5′- CCTTCAACGTCAGCGACTT -3′. The scrambled shRNA sequence used is 5′- CCTAAGGTTAAGTCGCCCTCG -3′.

2.4 Immunohistochemistry

Kidneys were fixed in 10% neutral-buffered formalin and were paraffin embedded. For immunohistological analyses, we used 4 μm paraffin kidney sections with heat-induced antigen retrieval, as described elsewhere [19]. Kidney sections were blocked with 5% BSA for 1 h at room temperature, followed by incubation with mouse monoclonal human anti- ANO1 (ab190721, Abcam, USA) 1:500 dilution overnight at 4 °C. The negative control sections were stained by using IgG. The HRP-conjugated secondary antibodies (1:1000 dilution) were purchased from KPL Inc. (Gaithersburg, MD, USA). Peroxidase substrates were diaminobenzidine (DAB) (Vector Laboratories Inc., Burlingame, CA, USA). The nuclei were counter-stained with hematoxylin (Vector Laboratories Inc.) for 2 min, and then were mounted, which were further analyzed by Axioplan microscope and AxioVision Rel.4.6. software (Zeiss, Jena, Germany). A minimum of 10 views per slide were captured and analyzed.

2.5 Confocal Immunofluorescence

Cells were cultured in DMEM/F-12 containing 10% FBS on glass coverslips and were starved when reaching 70% confluence. After 24–48 h, slides were fixed with ice-cold methanol or paraformaldehyde for 10 min, then were permeabilized and immune-stained with appropriate antibodies. For immunofluorescent staining, anti-ANO1 (diluted 1:500), anti-acetylated a-tubulin (diluted 1:1000, T7451, Sigma), anti-tubulin-detyrosinated (diluted 1:1000, AB3201, Sigma) and PC2 antibodies (diluted 1:200, provided by the Baltimore Polycystic Kidney Disease (PKD) Research and Clinical Core Center) were used. Binding of the primary antibody was visualized by incubation with secondary donkey anti-mouse antibodies conjugated with AlexaFluor 488 or 555 (1:1000 for each, Molecular Probes, Invitrogen, Darmstadt, Germany). IgG was used as negative controls. Confocal experiments were carried out on a Bio-Rad MRC-1024 laser scanning confocal microscope (Bio-Rad Laboratories, Hercules, CA, USA).

2.6 Real-Time PCR

Total RNA was isolated from *PKD1*$^{RC/RC}$ mouse, human kidney samples, transfected MDCK cells and *PKD1*$^{+/-}$ cells. The synthesis of cDNA was performed routinely by using the M-MLV Reverse Transcription system (Invitrogen Life Technologies, Darmstadt, Germany). Real-time RT–PCR was performed in a plate reader Light Cycler 480 by using a SYBR Green I (BioRad, USA) and a specific primer. The housekeeping gene GAPDH served as an internal control to estimate the relative quantity of mRNA expression and correct for differences in sample content. The following are primers used in this study: Human ANO1 primer sequences Forward, CAGCATGGAGATGTGTGACC; Reverse, CATCTGTTTCCGCTTCCAGT; Mouse ANO1 primer sequences Forward, GAAGCAACACCTATTCGACCTG; Reverse, TCCGTAACTTGCCCATTCCTC; Canis lupus ANO1 primer sequences Forward, AAAAGCAAAGAGAAGCGCCG; Reverse, GCCATGGCTGTCTTAACCCT.

2.7 D Laser Scanning Confocal Immunofluorescence

Three-dimensional structured illumination microscopy was performed using a standard protocol in our lab. Briefly, an ELYRA Super-resolution Microscopy system (Zeiss) equipped with an alpha 'Plan-Apochromat' 100_/1.46 Oil DIC oil immersion objective and an AndoriXon 885 EMCCD camera was used to capture raw images. Sections were acquired at 0.125-mm z-steps. Color channels were aligned using alignment parameters from control measurements with 0.5-mm diameter multispectral fluorescent beads (Zeiss). Structured illumination reconstruction and image processing were performed with the ZEN software package (Zeiss). Final image processing was performed by using Adobe Photoshop.

2.8 Western Blot Analysis

Protein was extracted by using the ProteoPrep® Total Extraction Sample Kit (Sigma, USA), and was measured with a BCA protein assay kit (Pierce, USA). Protein sample (60 μg) was loaded for acrylamide gel electrophoresis (SDS-PAGE, resolving gel concentration was 12%) and transferred to nitrocellulose membranes at 100 Volts for 2 h. The membrane was blocked by 5% non-fat milk for 1 h at room temperature. The membrane was probed at 4 °C over night with eight different primary antibodies: mouse anti-human ANO1 (diluted, 1:1000), rabbit anti-human PKD2 (1:1000, 07-488, Sigma), mouse anti-human ERK1/2 (1:2000, 4696#, Cell Signaling Technology), rabbit anti-human phospho-ERK1/2 (1:1000, 4376#, Cell Signaling Technology), rabbit anti-human STAT3 (1:1000, 12640#, Cell Signaling Technology), mouse anti-human phosphor-STAT3 (1:1000, 5726#, Cell Signaling Technology), mouse anti-human GAPDH (1:2000, 91153#, Sigma) and rabbit anti-mouse GAPDH (1:2000, 2118#, Cell Signaling Technology). After washing with PBS, the membrane was incubated with the corresponding HRP-labelled secondary antibody for 2 h at room temperature. Signals were developed by using the SuperSignal West Femto Luminol Enhanced ECL detection kit (Thermo Scientific). Visualization of protein bands was performed by using the ChemiDoc XRS imaging system (No.1708265, Bio-Rad, CA, USA). Band intensities were quantified by using ImageJ (National Institutes of Health, Washington D.C. USA).

2.9 D Collagen Gel Culture Assays

Cells were cultured with serum-free defined medium containing DMEM-F12 and insulin (5 μg/mL), transferrin (5 μg/mL), and selenium (ITS, Sigma, 5 ng/mL), penicillin, Streptomycin, and epidermal growth factor (Sigma, 25 ng/mL) to generate cysts. When reaching confluence, cells were trypsinized and 4000 cells suspended in 0.4 mL of ice-cold Minimum Essential Medium (MEM) containing collagen type I 2.9 mg/mL (BD Biosciences), 10 mM HEPES, 27 mM NaHCO3, penicillin, and Streptomycin. The cell suspension was placed onto one well of a 24-well plate. When the collagen was solidified, 1 mL of cell medium including 10 muM Forskolin was added to each well, and plates were maintained at 37 °C in a 5% CO_2 humidified atmosphere. After 2 weeks of treatment, cultured cysts were imaged under bright field illumination using the Nikon dissecting scope. Cyst diameters (with diameter $>$50 uM) were measured by using MetaMorph software (Molecular Devices, USA). At least 3 wells per group were measured.

2.10 Statistical Analyses

All data examined are presented as means $\pm$ SE. Comparisons between two groups were conducted using a two-tailed *t*-test when the data were normally distributed. *p* values of less than 0.05 were considered statistically significant. All analyses were carried out using GraphPad Prism software (GraphPad Software, USA), and all graphs were generated with the same software.

3. Results

3.1 ANO1 is Upregulated in Mouse and Human ADPKD Kidneys

To understand the transcriptional control of *Ano1* gene in kidneys, the renal expression of ANO1 was measured in hypomorphic $PKD1^{RC/RC}$ mice. In young 1-month-old mice without cysts, there is no difference in the expression of *Ano1* between WT and $Pkd1^{RC/RC}$ mice. Intriguingly, *Ano1* expression was significantly upregulated in adult $Pkd1^{RC/RC}$ mice after cystogenesis is initiated (Fig. 1A).

To examine if *ANO1* upregulation is relevant in ADPKD, we analyzed *ANO1* expression levels in human ADPKD kidneys (Fig. 1B). Western blotting analysis indicated that ANO1 was significantly upregulated almost 5 folds in human ADPKD kidneys as compared with normal controls (Fig. 1C,D). Immunohistochemical staining revealed strong staining of ANO1 in lining cells of cystic renal tubules, but not in normal tubules or glomeruli, of kidneys from ADPKD patients as compared with those from normal kidneys (Fig. 1E).

3.2 ANO1 Locates to Vesicles at the Ciliary Base but not Cilia Proper

We then assessed the subcellular localization of ANO1 in human renal collecting tubule epithelial (RCTE) cells by confocal immunofluorescence. As shown in Fig. 2A, contradictory to the assumption that ANO1 acts as a sensory receptor on the ciliary surface, ANO1 signal was only found at the ciliary base of RCTE cells. PKD1 deficiency did not change the localization of ANO1 (Fig. 2A). Moreover, we found that the intensity of ANO1 staining in the primary cilium of human $PKD1^{+/-}$ cells was stronger than that in RCTE cells (Fig. 2B). Super-resolution 3D structured illumination (SIM) microscopy analysis revealed that ANO1 was located to a subset of vesicles at the ciliary base in RCTE cells (Fig. 2C).

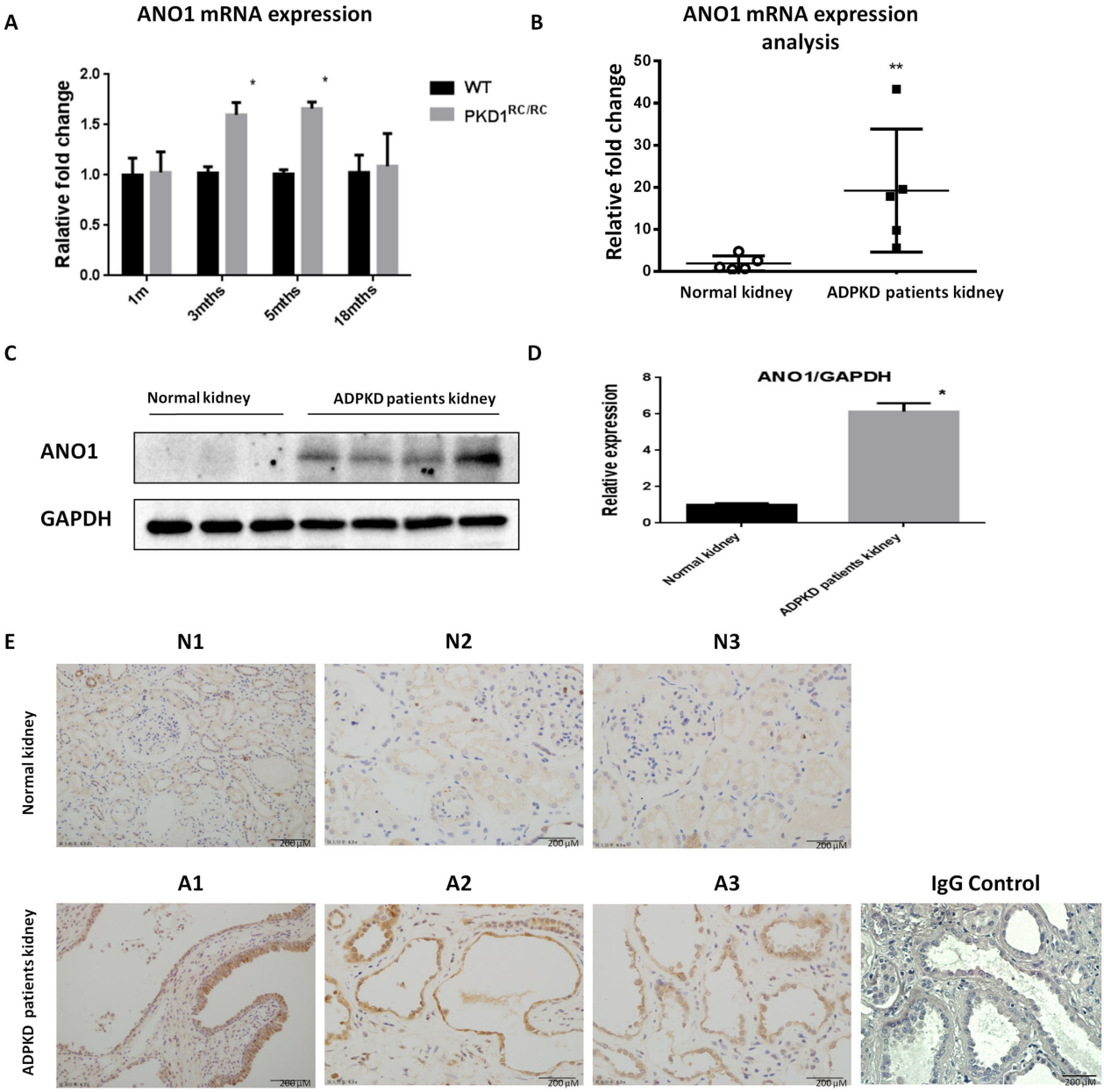

Fig. 1. ANO1 is up-regulated in mouse and human ADPKD kidneys. (A) Quantitative PCR analysis of ANO1 expression in kidney tissues of *PKD1*$^{RC/RC}$ mice with different ages (1, 3, 5, 18 months). (B) Quantitative PCR analysis of ANO1 expression in human normal control and ADPKD patients renal tissues. (C,D) Western blotting analysis of ANO1 expression in human normal control and ADPKD patients renal tissues and was further quantified. (E) Immunohistochemistry analysis of ANO1 (in brown) expression in human normal control (N1, N2, N3) and ADPKD patients (A1, A2, A3) renal tissues. IgG served as a negative control for staining. Scale bars, 200 μm. On representative result from three independent experiments was shown. *$p < 0.05$. **$p < 0.01$.

3.3 Knockdown of ANO1 Promotes Cilia Length and the Ciliary Dosage of Polycystin 2

To investigate the role of ANO1 in the context of cilia, we used siRNA to knock down the expression of *ANO1* in WT9-7 human *PKD1*$^{+/-}$ cells [20]. Contrary to previous discoveries that ANO1 deficiency reduces cilia length in IMCD3 cells [17], knock-down of *ANO1* in human PKD cells did not affect ciliogenesis, but instead caused a subtle increase in the cilium length (Fig. 3). Intriguingly, ANO1 deficiency significantly increased the ciliary dosage of polycystin 2. The effect of ANO1 on polycystin 2 expression was further studied by using ANO1 specific inhibitor Tinh16-A01 in a ADPKD cell line. The expression of polycystin 2 (PC2) was not affected by Tinh16-A01 (**Supplementary Fig. 1**).

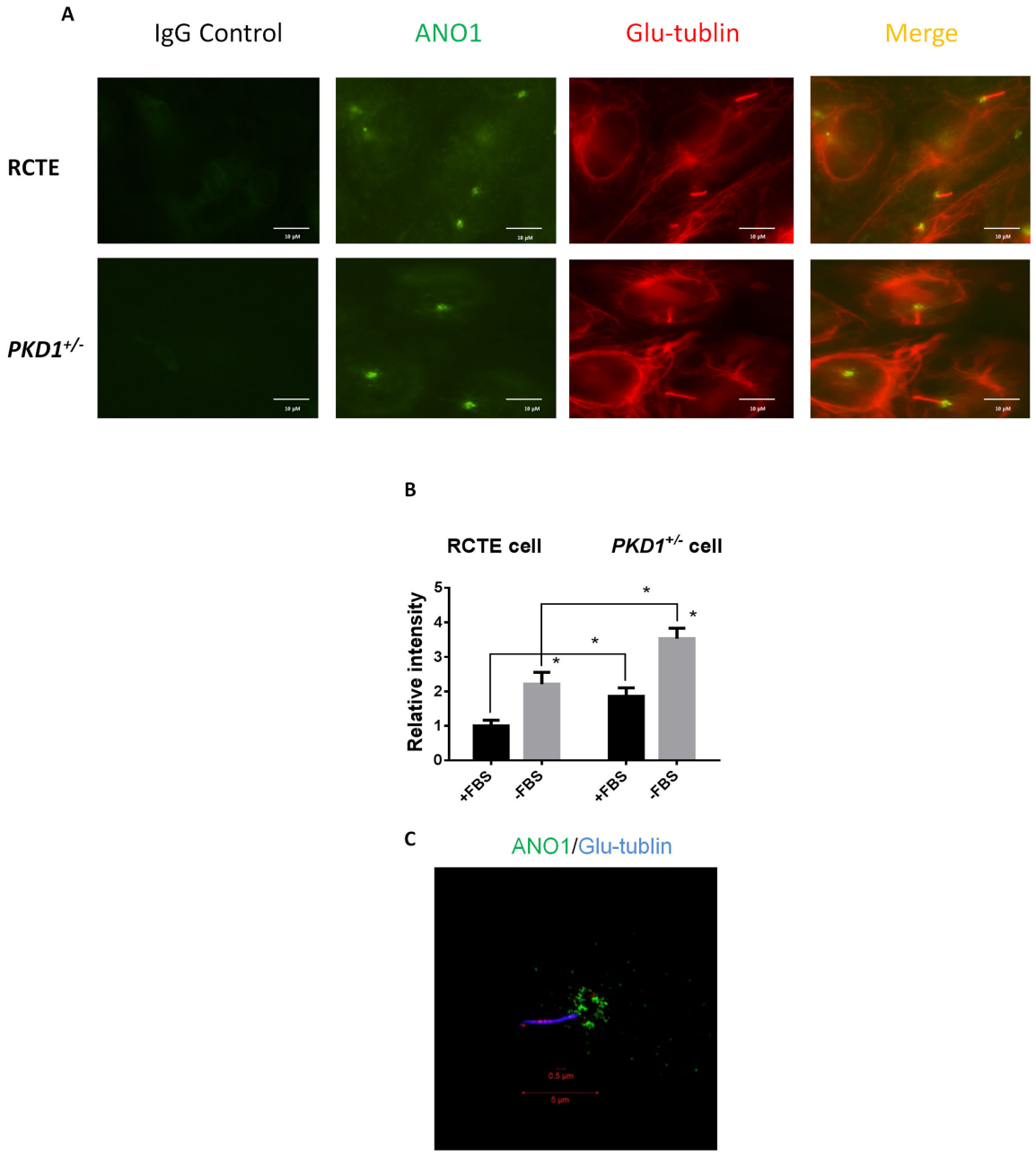

Fig. 2. ANO1 is localized in primary cilia. (A,B) Immunofluorescence staining for ANO1 and Glu-tubulin was performed on RCTE and ADPKD cells ($PKD1^{+/-}$ cells) and further quantitative analyzed by confocal microscopy. IgG was used as a negative control for staining on RCTE and $PKD1^{+/-}$ cells. Scale bars, 10 μm. (C) Super-resolution 3D structured illumination microscopy analysis of ANO1 in RCTE cells. On representative result from three independent experiments was shown.

3.4 Knock-Down of ANO1 Inhibits Cyst Formation in 3D-Culture Models

3D culture with MDCK or IMCD3 cells are classical *in vitro* models to study ADPKD [21]. ANO1 specific inhibitor Tinh16-A01 or Tannic acid was used to treat IMCD3 cells. Tinh16-A01 or Tannic acid significantly inhibited cyst formation in 3D-cultured IMCD3 cells (Fig. 4A,B). To further study the functional impact of ANO1 on renal cyst formation, we established MDCK cell line with steady knockdown of *Ano1* gene. As expected, genetic knockdown of *Ano1* significantly inhibited cyst formation in MDCK cells (Fig. 4C,D).

3.5 ANO1 Inhibition Corrects Abnormal Proliferative Pathways of ADPKD

We further examined the proliferative pathways abnormally upregulated in human PKD cells. *GANAB* is a novel ADPKD gene whose mutation compromises the protein maturity of PKD1 and PKD2 and impairs their ciliary

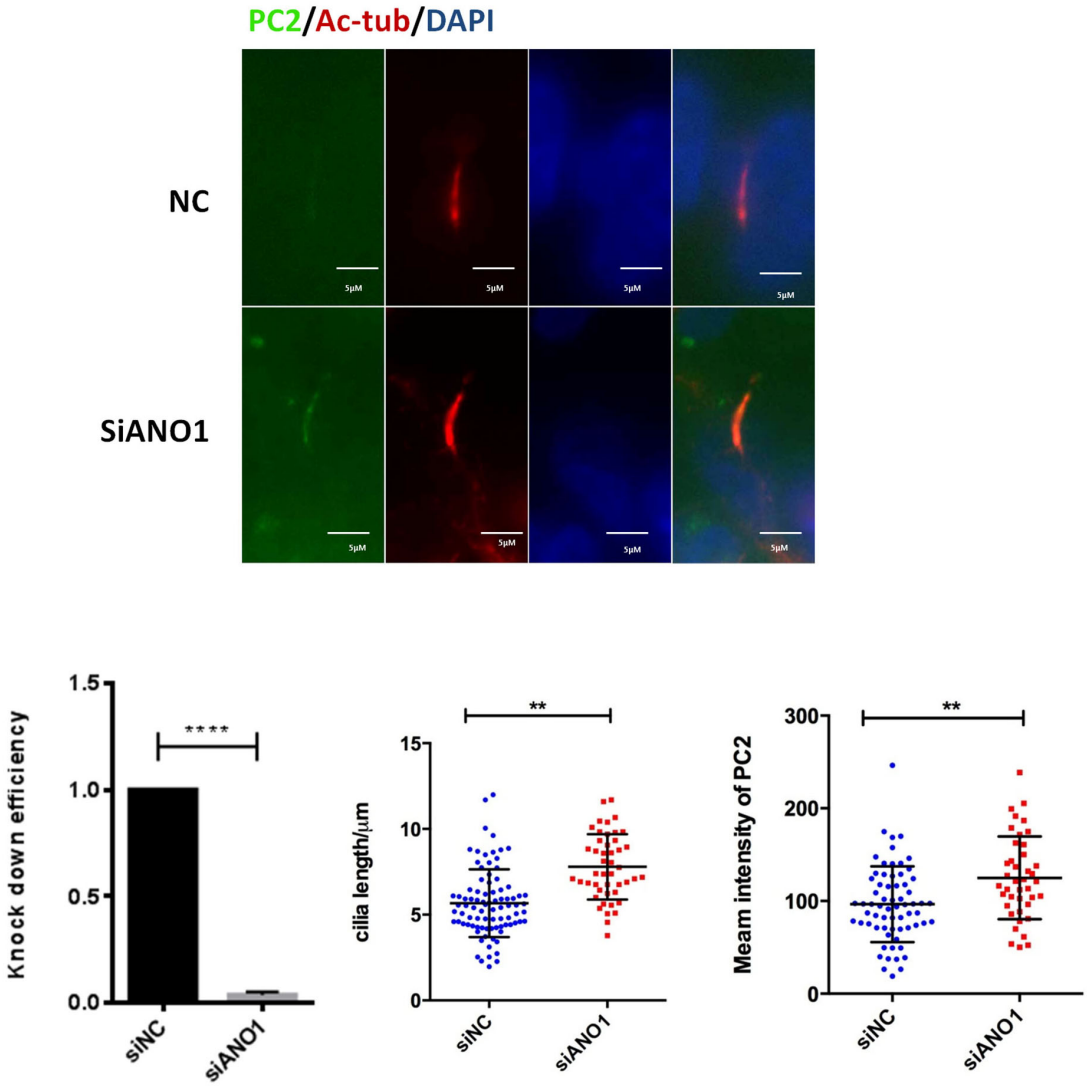

Fig. 3. Knockdown of ANO1 increases the cilium length and the expression of polycystin 2 (PC2). Immunofluorescence: nonsense control (NC) siRNA or siRNA against ANO1was transfected in human $PKD1^{+/-}$ cells. Immunofluorescence staining for PC2 and AC-tubulin was performed on RCTE and ADPKD cells ($PKD1^{+/-}$ cells) and further analyzed by confocal microscopy. Cilia length and intensity of PC2 were quantified. The knockdown efficiency of siRNA was determined by real-time PCR. On representative result from three independent experiments was shown. Scale bars, 5 μm. $^{**}p < 0.01$.

localization [22]. As shown in Fig. 5A, ANO1 inhibition by Tinh16-A01 subdued phosphorylation of STAT3 and ERK in human $GANAB^{-/-}$ renal collecting tubule epithelial (RCTE) cells. Tannic Acid treatment showed similar effects in a dose-dependent manner in $GANAB^{-/-}$ RCTE cells (Fig. 5B). We further examined the effect of ANO1 inhibition in $GANAB^{-/-}$ cells [21]. Knockdown of *ANO1* using two different siRNAs efficiently reduced activation of STAT3 and ERK pathways in $GANAB^{-/-}$ cells (Fig. 5C).

4. Discussion

ANO1 drives cyst growth in PKD models but with poorly understood molecular mechanisms [23]. In the current study, we confirmed that ANO1 is abnormally upregulated in cyst-lining cells in both human ADPKD kidneys and hypomorphic $Pkd1^{RC/RC}$ kidneys. ANO1 appears to be not an initiator of cystogenesis since its expression is not upregulated in pre-cystic (1 month) kidneys in $Pkd1^{RC/RC}$ mice. Instead, ANO1 expression is upregulated by defective polycystin signalings during cyst progression.

Although different lines of evidence suggested ANO1 deficiency impairs ciliogenesis, $Ano1^{-/-}$ mice show no hallmarks of classic ciliopathies, such as cystic disease, polydactyly, or situs inversus [24–26]. Kidney-specific knockout of ANO1 also shows no impact on ciliogenesis [26]. This is in line with our discovery that ANO1 deficiency is not detrimental to ciliogenesis but, instead, may promote cilia elongation or subdue cilia absorption by unclear mechanisms.

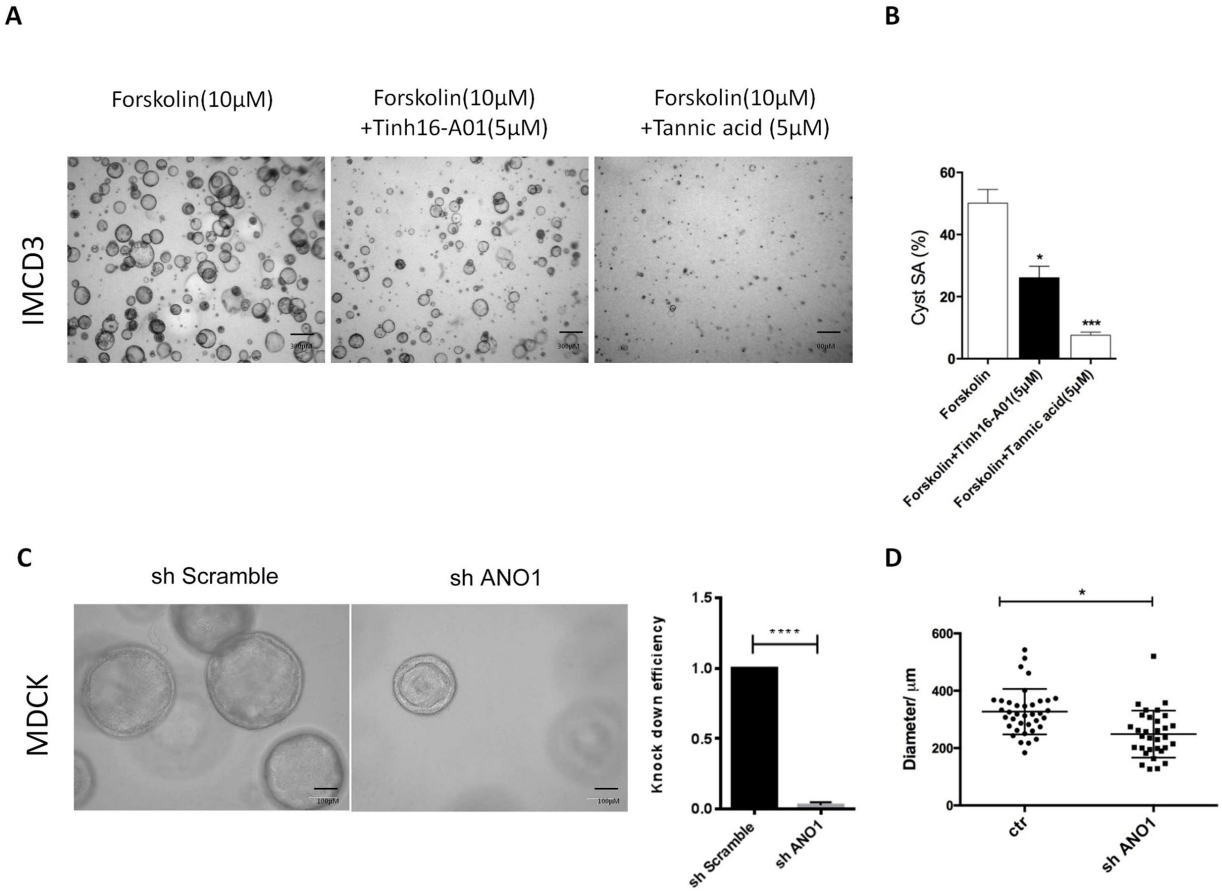

Fig. 4. Knock-down of ANO1 inhibits renal cyst formation in 3D culture models. (A,B) A three-dimensional (3D) culture model of cyst formation was established using IMCD3 cells which were treated with two different ANO1inhibitors (Tinh16-A01 or Tannic acid). After 2 weeks of culture, the Surface area of cysts (SA) was measured. Scale bars, 300 μm. (C,D) 3D culture model of cyst formation was established using MDCK cells which were transfected with shRNA against ANO1. Knock down efficiency was measured by RT-PCR before MDCK cells were planted into the collagen gel. After 2 weeks of culture, the diameter of cysts was measured. On representative result from three independent experiments was shown. Scale bars, 100 μm. *$p < 0.05$. ***$p < 0.01$.

PC2 is localized to the primary cilium of tubular cells and ciliary exclusion of PC2 promotes renal cystogenesis in ADPKD model [27]. It has been reported that the length of PC2-negative cilia is significantly shorter than that of PC2-positive cilia [28]. We hypothesized that ANO1 inhibits cilium formation through increasing PC2 content in the primary cilium. Here, we showed that knock-down of ANO1 increased the cilia length which was correlated with increased expression of PC2 in the primary cilium of ADPKD cells. While ANO1 inhibited is not decrease expression of PKD2 in the GANAB cells.

Previous study showed that ANO1 was localized to the cilia of mature olfactory sensory neurons [29]. In our hand, we could not detect the ciliary localization for ANO1 even by using super-resolution SIM microscopy analysis. ANO1 is specifically restricted to a subset of vesicles at the ciliary base, suggesting that ANO1 is not used by renal epithelial cells as a sensory receptor or chloride channel on the cilia surface to regulate signal transduction and/or ion exchange between renal epithelia and tubular fluids. It is thus interesting how ANO1 regulates ion homeostasis and cilia-related function at the ciliary base in the context of ADPKD. One plausible mechanism is that ANO1 may regulate the ciliary import or removal of key molecules involved in cilia formation and function by influencing local ion homeostasis and/or vesicle dynamics, as is evidenced by upregulation of PC2 and increased cilia length in ANO1-deficient cells. ANO1 deficiency may lead to enhanced trafficking of vesicles targeted to cilia. A line of evidence supporting this hypothesis is the electron microscopy study of proximal tubular cells in $Ano1^{-/-}$ mouse kidneys, which revealed an accumulation of endosomal vesicles at the apical surface of renal cells [30]. Considering ANO1 is a calcium-activated chloride channel, its activity in the subset of ciliary vesicles could be reciprocally affected by polycystin-mediated calcium signaling in the context of cilia. It is thus intriguing to study how polycystins and ANO functionally crosstalk at the molecular level to regulate ion homeostasis at the

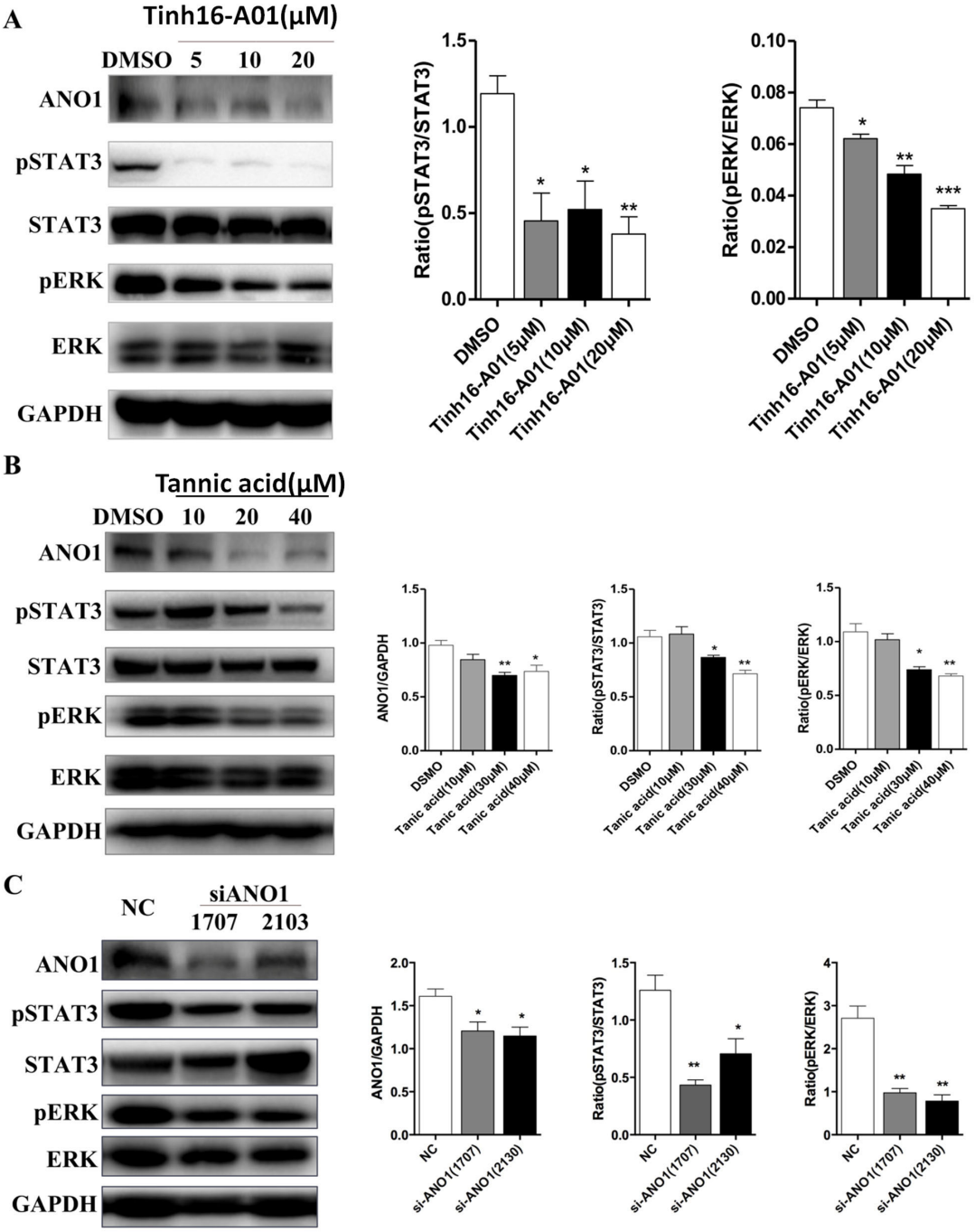

Fig. 5. The effect of ANO1 on cell proliferation signaling pathways of ADPKD. (A) *GANAB* cells was treated with ANO1 specific inhibitor Tinh16-A01.The expression of ANO1 and phosphorylation of STAT3 and ERK in *GANAB* cells were analyzed by Western blot and further quantified. (B) *GANAB* cells was treated with ANO1 specific inhibitor Tannic acid. The expression of ANO1 and phosphorylation of STAT3 and ERK in *GANAB* cells were analyzed by Western blot and further quantified. (C) *GANAB* (an ADPKD cell line) cells were transfected with nonsense control (NC) siRNA or two different siRNAs against ANO1. The expression of ANO1 and phosphorylation of STAT3 and ERK in *GANAB* cells were analyzed by Western blot and further quantified. $*p < 0.05$. $**p < 0.01$.

ciliary base and determine proper cilia trafficking of key molecules, as well as the implications in ADPKD.

ADPKD is characterized by activation of multiple proliferating signaling pathways such as STAT3 and ERK pathways [31]. It has been reported that ANO1 promotes cyst growth by increasing cystic epithelial cell proliferation [32]. Thus, we hypothesized that ANO1 promotes cyst growth by activating STAT3 and ERK proliferating pathways. We first confirmed ANO1 inhibitors reduced cyst size in two 3D culture models. Next, we showed

that activation of STAT3 and ERK proliferating pathways in GANAB$^{-/-}$ cells were dose-dependently inhibited by two different ANO1 inhibitors. We further knocked down ANO1 gene in another ADPKD cells and we showed that phosphorylation of STAT3 and ERK were reduced by ANO1 siRNAs. The limitation of this study is that cell proliferation assay was not performed to further show the pro-proliferative effect of ANO1.

5. Conclusions

Our data indicate ANO1 is a negative regulator for both cilia length and cilia trafficking of polycystin-2 and provide mechanistic insights regarding the therapeutic potential of ANO1 pathway in ADPKD treatment.

Author Contributions

CM and TX conceived and supervised the study; TX and JH designed experiments; TX, MC, QX, LF, and KL performed experiments; TX provided new tools and reagents; TX and MC analysed data; TX, CX and JH wrote the manuscript; JH and CX made manuscript revisions.

Ethics Approval and Consent to Participate

Not applicable.

Acknowledgment

Not applicable.

Funding

This study was supported by grants from the national key research and development program of china (2016yfc0901502), the national natural science foundation of china (no. 81873595, 81670612, 81300560), shanghai municipal key clinical specialty (shslczdzk02503) and pujiang talent program of shanghai, china (no. 17pj1407700).

Conflict of Interest

The authors declare no conflict of interest.

Supplementary Material

Supplementary material associated with this article can be found, in the online version, at https://doi.org/10.31083/j.fbl2707216.

References

[1] Laleye A, Awede B, Agboton B, Azonbakin S, Biaou O, Sagbo G, *et al*. Autosomal dominant polycystic kidney disease in University Clinic of Nephrology and Haemodialysis of Cotonou: clinical and genetical findings. Genetic Counseling. 2012; 23: 435–445.

[2] Ghata J, Cowley BD Jr. Polycystic Kidney Disease. Comprehensive Physiology. 2017; 7: 945–975.

[3] Mangolini A. Role of calcium in polycystic kidney disease: from signaling to pathology. World Journal of Nephrology. 2016; 5: 76–83.

[4] Hu J, Harris PC. Regulation of polycystin expression, maturation and trafficking. Cellular Signalling. 2020; 72: 109630.

[5] Rodat-Despoix L, Delmas P. Ciliar functions in the nephron. Pflugers Archiv European Journal of Physiology. 2009; 458: 179–187.

[6] Ma M. Cilia and polycystic kidney disease. Seminars in Cell & Developmental Biology. 2021; 110: 139–148.

[7] Su X, Wu M, Yao G, El-Jouni W, Luo C, Tabari A, *et al*. Regulation of polycystin-1 ciliary trafficking by motifs at its C-terminus and polycystin-2 but not by cleavage at the GPS site. Journal of Cell Science. 2015; 128: 4063–4073.

[8] Menezes LF, Germino GG. The pathobiology of polycystic kidney disease from a metabolic viewpoint. Nature Reviews Nephrology. 2019; 15: 735–749.

[9] Hopp K, Ward CJ, Hommerding CJ, Nasr SH, Tuan H, Gainullin VG, *et al*. Functional polycystin-1 dosage governs autosomal dominant polycystic kidney disease severity. Journal of Clinical Investigation. 2012; 122: 4257–4273.

[10] Bhoonderowa L, Hameurlaine F, Arbabian A, Faqir F, Amblard F, Coscoy S. Polycystins and intercellular mechanotransduction: a precise dosage of polycystin 2 is necessary for alpha-actinin reinforcement of junctions upon mechanical stimulation. Experimental Cell Research. 2016; 348: 23–35.

[11] Lee SH, Somlo S. Cyst growth, polycystins, and primary cilia in autosomal dominant polycystic kidney disease. Kidney Research and Clinical Practice. 2014; 33: 73–78.

[12] Li A, Tian X, Zhang X, Huang S, Ma Y, Wu D, *et al*. Human Polycystin-2 Transgene Dose-Dependently Rescues ADPKD Phenotypes in Pkd2 Mutant Mice. The American Journal of Pathology. 2015; 185: 2843–2860.

[13] Buchholz B, Faria D, Schley G, Schreiber R, Eckardt K, Kunzelmann K. Anoctamin 1 induces calcium-activated chloride secretion and proliferation of renal cyst-forming epithelial cells. Kidney International. 2014; 85: 1058–1067.

[14] Jang Y, Oh U. Anoctamin 1 in secretory epithelia. Cell Calcium. 2014; 55: 355–361.

[15] Danahay H, Gosling M. TMEM16A: An Alternative Approach to Restoring Airway Anion Secretion in Cystic Fibrosis? International Journal of Molecular Sciences. 2020; 21: 2386.

[16] Cabrita I, Kraus A, Scholz JK, Skoczynski K, Schreiber R, Kunzelmann K, *et al*. Cyst growth in ADPKD is prevented by pharmacological and genetic inhibition of TMEM16a in vivo. Nature Communications. 2020; 11: 4320–4333.

[17] Ruppersburg CC, Hartzell HC. The Ca2+-activated Cl- channel ANO1/TMEM16A regulates primary ciliogenesis. Molecular Biology of the Cell. 2014; 25: 1793–1807.

[18] He M, Ye W, Wang WJ, Sison ES, Jan YN, Jan LY. Cytoplasmic Cl(-) couples membrane remodeling to epithelial morphogenesis. Proceedings of the National Academy of Sciences of the United States of America. 2017; 114: E11161–E11169.

[19] Kuloglu T, Aydin S. Immunohistochemical expressions of adropin and inducible nitric oxide synthase in renal tissues of rats with streptozotocin-induced experimental diabetes. Biotechnic and Histochemistry. 2014; 89: 104–110.

[20] Loghman-Adham M, Nauli SM, Soto CE, Kariuki B, Zhou J. Immortalized epithelial cells from human autosomal dominant polycystic kidney cysts. American Journal of Physiology-Renal Physiology. 2003; 285: F397–F412.

[21] Cornec-Le Gall E, Torres VE, Harris PC. Genetic Complexity of Autosomal Dominant Polycystic Kidney and Liver Diseases. Journal of the American Society of Nephrology. 2018; 29: 13–23.

[22] Porath B, Gainullin VG, Cornec-Le Gall E, Dillinger EK, Heyer CM, Hopp K, *et al*. Mutations in GANAB, Encoding the Glucosidase IIalpha Subunit, Cause Autosomal-Dominant Polycystic Kidney and Liver Disease. American Journal of Human Genetics. 2016; 98: 1193–1207.

[23] Schreiber R, Buchholz B, Kraus A, Schley G, Scholz J, Ousingsawat J, *et al*. Lipid Peroxidation Drives Renal Cyst Growth In Vitro through Activation of TMEM16A. Journal of the American Society of Nephrology. 2019; 30: 228–242.
[24] Rock JR, Futtner CR, Harfe BD. The transmembrane protein TMEM16a is required for normal development of the murine trachea. Developmental Biology. 2008; 321: 141–149.
[25] Billig GM, Pál B, Fidzinski P, Jentsch TJ. Ca2+-activated Cl- currents are dispensable for olfaction. Nature Neuroscience. 2011; 14: 763–769.
[26] Schenk LK, Buchholz B, Henke SF, Michgehl U, Daniel C, Amann K, *et al*. Nephron-specific knockout of TMEM16a leads to reduced number of glomeruli and albuminuria. American Journal of Physiology-Renal Physiology. 2018; 315: F1777–F1786.
[27] Ma M, Gallagher A, Somlo S. Ciliary Mechanisms of Cyst Formation in Polycystic Kidney Disease. Cold Spring Harbor Perspectives in Biology. 2017; 9: a028209.
[28] Xu C, Rossetti S, Jiang L, Harris PC, Brown-Glaberman U, Wandinger-Ness A, *et al*. Human ADPKD primary cyst epithelial cells with a novel, single codon deletion in the PKD1 gene exhibit defective ciliary polycystin localization and loss of flow-induced Ca2+ signaling. American Journal of Physiology-Renal Physiology. 2007; 292: F930–F945.
[29] Maurya DK, Menini A. Developmental expression of the calcium-activated chloride channels TMEM16a and TMEM16B in the mouse olfactory epithelium. Developmental Neurobiology. 2014; 74: 657–675.
[30] Faria D, Rock JR, Romao AM, Schweda F, Bandulik S, Witzgall R, *et al*. The calcium-activated chloride channel Anoctamin 1 contributes to the regulation of renal function. Kidney International. 2014; 85: 1369–1381.
[31] Ye H, Wang X, Constans MM, Sussman CR, Chebib FT, Irazabal MV, *et al*. The regulatory 1α subunit of protein kinase a modulates renal cystogenesis. American Journal of Physiology-Renal Physiology. 2017; 313: F677–F686.
[32] Guo S, Chen Y, Pang C, Wang X, Qi J, Mo L, *et al*. Ginsenoside Rb1, a novel activator of the TMEM16A chloride channel, augments the contraction of guinea pig ileum. Pflugers Archiv European Journal of Physiology. 2017; 469: 681–692.